

Visible Emission from Hexagonal Boron Nitride Nanosheets upon Molecular Doping

A Thesis

Submitted to
Indian Institute of Science Education and Research
Pune in Partial Fulfillment of the Requirements for the
BS-MS Dual Degree

Programme by

Vikash Kumar



Indian Institute of Science Education and Research
Pune, India

March, 2018

Supervisor: Dr. Nirmalya Ballav

Department of Chemistry

IISER Pune

Certificate

This is to certify that this dissertation entitled “**Visible Emission from Hexagonal Boron Nitride Nanosheets upon Molecular Doping**” towards the partial fulfillment of the BS-MS dual degree programme at the Indian Institute of Science Education and Research, Pune represents original research carried out by **Vikash Kumar at Indian Institute of Science Education and Research, Pune** under the supervision of **Dr. Nirmalya Ballav**, Department of Chemistry, Indian Institute of Science Education and Research, Pune during the academic year 2017-2018.


Dr. Nirmalya Ballav 20/3/2018

(Supervisor)

Associate Professor

Department of Chemistry, IISER Pune

Email: nballav@iiserpune.ac.in

Signature:



Vikash Kumar

20131011

IISER Pune

Declaration

I hereby declare that the thesis entitled “**Visible Emission from Hexagonal Boron Nitride Nanosheets upon Molecular Doping**” submitted for the fulfilment of the BS-MS dual degree programme at Indian Institute of Science Education and Research (IISER), Pune has not been submitted by me to any other University or Institution. This work was carried out at the Indian Institute of Science Education and Research (IISER), Pune India under the supervision of Dr. Nirmalya Ballav.


Dr. Nirmalya Ballav 20/3/2018

(Supervisor)

Associate Professor

Department of Chemistry, IISER Pune

Email: nballav@iiserpune.ac.in

Signature:



Vikash Kumar

20131011

IISER Pune

Dedicated to my Parents

Acknowledgments

First of all, I would like to express my sincere gratitude to my thesis supervisor **Dr. Nirmalya Ballav** for giving me a chance to work in his lab from my second year. Starting from his guidance, to the freedom to work in the lab in all these years, and letting me figure things out on my own, he has been a huge help. His down to earth and friendly nature has not only helped me to be a good researcher but also a good human being, something that I consider a very valuable lesson. Sir's guidance and timely inputs have helped me to come a long way and will continue to help me in the future as well.

I would also like to thank my TAC member **Dr. Pramod Pillai** for supporting me throughout my undergraduation and giving me advice regarding my research whenever necessary. Also, I would like to acknowledge **Dr. Musthafa Muhammed** for supporting me in my lab theory project and giving me valuable suggestions regarding my projects as well as my coursework. I would like to extend my thanks to the IISER Pune Faculty for their excellent teaching which helped me in developing interest in science and research.

I owe a huge thanks to my lab senior **Dr. Barun Dhara** and **Mr. Plawan Kumar Jha**. I will always be indebted for their inspiring guidance, timely criticism, and all the pragmatic suggestions. They have been a huge motivation for me and their dedication towards research and the work they do will always inspire me. Their suggestions, throughout my fifth year, as well as the years preceding it have helped me figure out the solutions of the problems I came across and helped me work in a systematic way.

A special shout out to all my lab mates Dr. Rajendra Ranguwar, Mr. Shammi Rana, Ms. Kriti Gupta, Dr. Syed Zahid Hassan, Ms. Debashree Roy, Mr. Anupam Prasoon, Ms. Ashwini Jadhav, Mr. Jainendra Singh and many more for all their co-operation and friendly attitude throughout which helped me execute my work in a much better way.

My friends Priyanshu Chandra, Dheerendra Singh Rajput, Atul Chaudhary, Nitin Kumar, Ankit Kumar, Abhishek Kumar, Sudhir Kumar, Anand Kumar, Abhishek Mishra, Reman Kumar, and many more at IISER have been like a family all these years. It goes without saying that I am immensely thankful to all of them and their invaluable friendship.

The acknowledgements are incomplete without expressing my heartfelt thanks to my Mummy, Papa and my brother who have been my support systems and my biggest mentors. I am here today because of what they made me, and I can't ever thank them enough for all that they have done for me. Along with my family, I would like to express my gratitude towards my high school teachers, especially Mr. Pushkar Srigyan and Mr. Dharmendra Kumar for making me the person I am today.

Last but not the least, I would like to thank DST-INSPIRE and Infosys Foundation for providing me the fellowship throughout my years in IISER. The financial aid has indeed helped me achieve my dreams.

Vikash Kumar.

Contents

Abstract.....	9
Chapter 1.....	9-27
1.1 Introduction.....	9-11
1.2 Materials and Methods.....	11-12
1.2.1 List of Chemicals.....	11
1.2.2 Exfoliation Process of BN.....	11
1.2.3 Synthesis of BN-TCNQ.....	12
1.2.4 Synthesis of Na-DCTC.....	12
1.2.5 Synthesis of BN-DCTC.....	12
1.3 Structure of BN, TCNQ, BN-TCNQ.....	12
1.4 Characterization.....	13
1.5 Results and Discussion.....	13-18
1.6 Mechanism.....	18-22
1.6.1 Conversion of TCNQ to DCTC.....	18
1.6.1 Experiment 1.....	19
1.6.2 Experiment 2.....	19-20
1.6.3 Experiment 3.....	20-21
1.6.4 Experiment 4.....	21
1.6.5 Experiment 5.....	22
1.7 Detailed Investigation.....	22-24
1.7.1 Concentration dependent studies.....	22
1.7.2 Temperature dependent studies.....	23
1.7.3 Laser bleaching effect.....	23-24
1.8 Electrical Measurement.....	24
1.9 Conclusion.....	25
2.0 Bibliography.....	26-27

List of Schemes/Figures

Scheme 1: Interaction of TCNQ with BN

Scheme 2: Chemical conversion of TCNQ to DCTC

Figure 1: Synthesis of BN-TCNQ hybrid

Figure 2: Characterization of BN, TCNQ, BN-TCNQ via PXRD, Raman and AFM

Figure 3: FESEM and XPS of BN-TCNQ

Figure 4: Solid state UV, Photoluminescence and confocal images of BN, TCNQ,
BN-TCNQ

Figure 5: FTIR spectra of BN, TCNQ, BN-TCNQ

Figure 6: CV spectra of BN-TCNQ supernatant solution

Figure 7: UV-vis. and Raman spectra

Figure 8: Confocal image and FTIR spectra

Figure 9: Confocal image of BN-DCTC

Figure 10: Electrical measurement, and Tauc plot of BN, TCNQ, BN-TCNQ

Abstract

The photoluminescence (PL) properties are the most promising for optoelectronic devices. However, achieving PL in hexagonal boron nitride (BN) is challenging. Here, we have mixed BN with 7,7,8,8-Tetracyanoquinodimethane (TCNQ) to produce a BN-TCNQ complex. Interestingly, the BN-TCNQ complex showed photoluminescence (PL) properties, which may be attributed to the charge transfer between BN and TCNQ. Moreover, the detail technical investigation of the reaction mixture revealed that the TCNQ first converts into α,α -dicyano-p-toluoyl cyanide anion (DCTC⁻), and then interacts with BN sheet, which is ultimately responsible for the PL characteristics. The DC electrical conductivity of the BN-TCNQ complex is enhanced ~2 fold compared to BN, which is mainly because of the decreased band gap of the complex, and also corroborates the efficient charge transfer phenomenon. Our approach can be a valuable example in terms of modulating the optical and electrical properties in two dimensional materials concerning the enhancement of optoelectronic properties and pave the way to develop devices for industrial applications.

1.1 Introduction

On peeling off bulk three dimensional (3D) layered materials, an atomically thin 2D sheet is obtained. Van der Waals is the force of attraction between the sheets which has to be overcome for getting a single layered 2D material.¹ The overall composition remains same while the dimension changes on going from 3D to 2D, complementing a new set of properties and applications which are absent in bulk (3D).¹⁻³ This observation is attributed to the change in band alignment.⁴ The dimension-property correlation is well known since a long time, however, in the domain of 2D materials it was only in 2004 when scientists Novoselov and Geim discovered single layer of graphene (a hexagonal form of carbon with sp^2 hybridization) for the first time using simple scotch tape method.⁵ Since then an enormous interest has been triggered in this field owing to their unbeatable properties such as high carrier mobilities⁵, superconductivity⁶, mechanical flexibility⁷, good thermal

conductivity, as well as high optical and UV absorption² giving rise to myriad of applications such as in electronics, valleytronics, catalysis and biosensing.¹⁻² In the last few decades, a plethora of 2D materials have been experimentally realized and lots more are on the way, as predicted theoretically.⁸ Some other well known 2D materials discovered after graphene are transition-metal dichalcogenides (TMDCs) (MoS_2 , WS_2 , WSe_2), and hexagonal boron nitride (BN) covering a wide range of band gap (~ 0 eV to ~ 6 eV).¹ Plenty of methods are available such as CVD (Chemical Vapor Deposition), PVD (Physical Vapor Deposition), ALD (Atomic Layer deposition), sonication assisted liquid phase exfoliation, chemical route to prepare the single 2D sheets from their bulk counterpart.^{2, 9}

Hexagonal boron nitride (BN), a member of the 2D family, is isoelectronic and has similar crystal lattice as graphene.² The presence of ionicity in BN localizes the electronic states and breaks its symmetry resulting in a large band gap (~ 6 eV) but in addition, supplements to its excellent thermal and chemical stability.^{2, 10} BN has been mainly used as lubricants, nanofillers and as a dielectric to supply gate voltage in field effect transistors (FETs).¹⁰⁻¹¹

In last few decades, Photoluminescence (PL) properties of BN have attracted a great attention in the scientific community.¹²⁻¹³ Since BN has a wide band gap it can host optically active defects, giving rise to luminescence properties.¹⁴ Luc et al. showed that UV laser irradiation can induce PL properties; the observation was assigned to impurity and mono or multiple nitrogen vacancies.^{13, 15} Trang et al. also showed quantized emission phenomenon in monolayer and multilayer BN which gets generated by thermal treatment at 850°C .¹⁶ Another approach to engineer the defect of thermally treated BN flakes was also carried out by ion implantation or laser ablation employed for improving the emission properties of BN.¹⁴⁻¹⁵ The reasoning behind the emission phenomenon is debatable, however color centre (defects and impurities) till now is mostly adopted reason for such emission phenomenon.^{13, 16-17} The mentioned method to engineer the BN PL properties requires harsh conditions such as thermal treatment, laser irradiation and ion implantation.^{12, 14}

Doping method is another well known adopted approach since a long time for engineering band gap resulting in new physicochemical properties. Hetero-atom such as carbon,

oxygen, fluorine doping in hexagonal boron nitride (BN) are able to create defect/impurity states that enables a plethora of applications in optical, electronic and magnetic domains.^{2, 18-19} Molecular doping is also shown to engineer the band gap. Researchers have doped small organic molecules such as in TCNQ, F₄-TCNQ (fluorinated TCNQ) in molybdenum disulfide (MoS₂), tungsten disulfide (WS₂) to tune their PL properties.²⁰⁻²¹ Theoretical prediction on molecular charge transfer between BN and donor/acceptor organic molecule such as TCNQ/TTF (tetrathiafulvalene) is known to happen via π - π interaction, however, experimental realization is still lacking.²²⁻²³

Here for the first time, we attempted to explore the charge transfer phenomenon between BN and TCNQ via wet chemical method. We have fully characterized the BN-TCNQ hybrid and found interesting results: (1) PL property and (2) enhanced electrical conductivity. It is well known that TCNQ can exist in three redox active forms, where one of its form can be chemically converted to DCTC⁻. From the extensive experimental investigation, we proposed the interaction of DCTC⁻ with BN justifying the emergence of aforementioned properties. The new concept of molecular doping in BN opens a new path for optoelectronic applications.

1.2 Materials and Methods

1.2.1 Chemicals

hexagonal boron nitride (BN) (1 μ m, 98%), TCNQ were purchased from Sigma-Aldrich. Sodium nitrite (NaNO₂) was purchased from TCI. IPA (Isopropyl Alcohol), DMF (*N,N*-Dimethylformamide), Acetone, Water were used as solvents.

1.2.2 Exfoliation Process

BN powder (450 mg) was taken in a conical flask and 150 ml of co-solvent IPA:water (1:1) was added into it.²⁴ The solution was sonicated in sonication bath with the frequency of 40 kHz for 4.5 hr at RT. The resulting dispersion was centrifuged at 1000 r.p.m. for 10 min, then the supernatant was collected followed by another centrifugation at 4000 r.p.m. for 10 min to further remove non-exfoliated BN. The obtained supernatant solution was labeled as BN-Exf. and used for further experiments.

1.2.3 Synthesis of BN-TCNQ

BN-Exf. (10 ml) and TCNQ (1 mM) in 10 ml DMF were mixed and kept in a beaker for 2 weeks and the pink coloured precipitate settled down. The pink precipitate was washed once with DMF and then dried at 90 °C. The powder was labeled as BN-TCNQ.

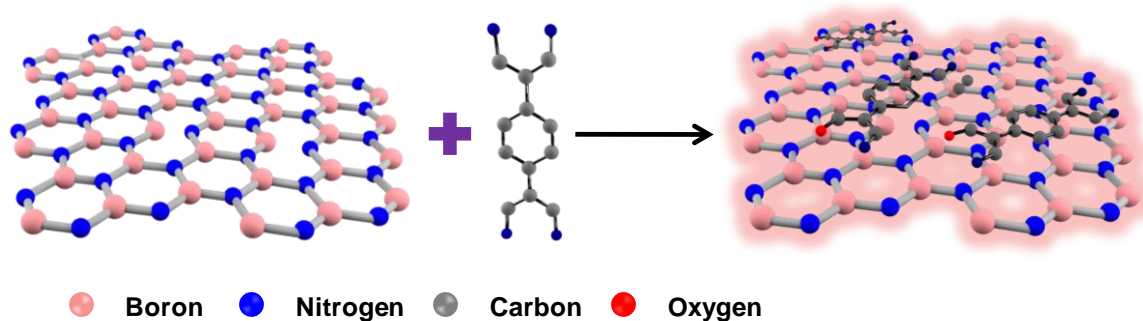
1.2.4 Synthesis of Na-DCTC

Sodium nitrite (NaNO_2) (5.2 mmol) was dissolved in water (16 ml) and added into warm solution of acetone (200 ml) containing TCNQ (2.96 mmol). The resulting dark red solution was evaporated and Na-DCTC powder was obtained.²⁵

1.2.5 Synthesis of BN-DCTC

BN-Exf. (60 ml) taken in a vial and Na-DCTC (6ml) was added to it and the solution was stirred and heated at 120 °C for 6 hr. The resulting precipitate was collected, dried at 90 °C and used for further experiments.

1.3 Structure



Scheme 1: schematic of BN, TCNQ and BN-TCNQ.

1.4 Characterization

PXRD data was collected on a Bruker D8 Advance diffractometer with Cu K α radiation ($\lambda = 1.5406 \text{ \AA}$) varying 2θ from 5 to 50°. FTIR spectra were collected from a NICOLET 6700 spectrophotometer with KBr pellets from 400 to 4000 cm^{-1} with a resolution of 4 cm^{-1} . Solid-state UV-vis. spectra were obtained from Perkin Elmer Lambda 950 spectrometer. The photoluminescence studies were performed on a Fluorolog-3 spectrofluorometer (HORIBA Scientific). Samples were dispersed in DMF, followed by drop casting on clean silicon wafer; then, morphological features was performed by using a field-emission scanning electron microscope (FESEM Carl-Zeiss Ultra). Raman spectra ($\lambda_{\text{ex.}} = 488 \text{ nm}$) recorded at Raman microscope (LabRAM HR, Horbia Jobin Yvon) with a 20 \times objective lens. The direct current (DC) conductivity was measured by two-probe technique MODEL 4200-SCS Semiconductor Characterization System.

1.5 Results and Discussion

BN was exfoliated via sonication method as reported in literature.²⁴ The resulting dispersed BN solution (BN-Exf.) was dried and characterized using different techniques such as PXRD, AFM, and Raman spectroscopy. The schematic of exfoliation processes and BN-TCNQ hybrid synthesis is shown in [Figure 1](#).

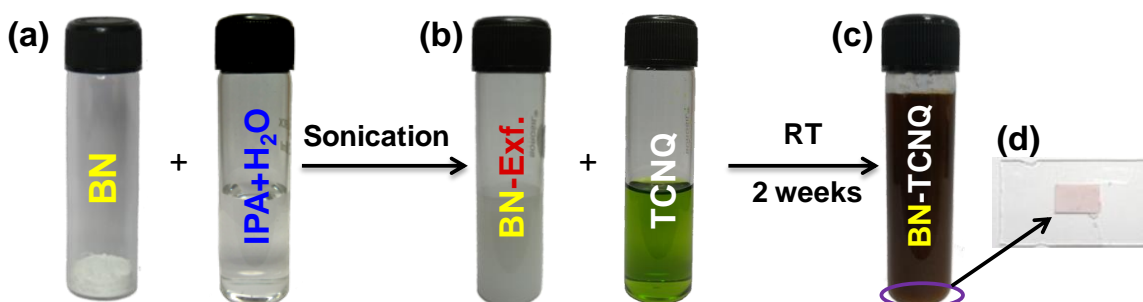


Figure 1: IPA:water solvent added in BN powder (a), BN-Exf. dispersed solution added in TCNQ (DMF) (b), BN-TCNQ hybrid after 2 weeks (c), Pink precipitate of BN-TCNQ (d).

The structure of BN-Exf. was investigated by powder X-ray diffraction (PXRD). As shown

in Figure 2a, the main characteristic diffraction peak can be observed at 26.4° arising from (002) plane, compared with the BN, the (002) peaks of BN-Exf. shows a remarkably reduced intensity indicating the presence of thin BN sheets and much less extended/ordered stacking in the c direction.¹¹ The PXRD of BN-TCNQ matches with BN indicating structural integrity after the hybrid formation. The Raman spectra (Figure 2b) were collected using 488 nm laser. BN shows a peak at 1364.9 cm^{-1} that can be assigned to B-N E_{2g} vibrational mode. A blue shift to 1365.4 cm^{-1} for BN-Exf. is consistent with reported literature.¹² Note that in BN-TCNQ the Raman shift is 1364.9 cm^{-1} similar to BN, this is because BN-TCNQ has 22-24 layer stacked together so it behaves as BN, and cannot be distinguished.

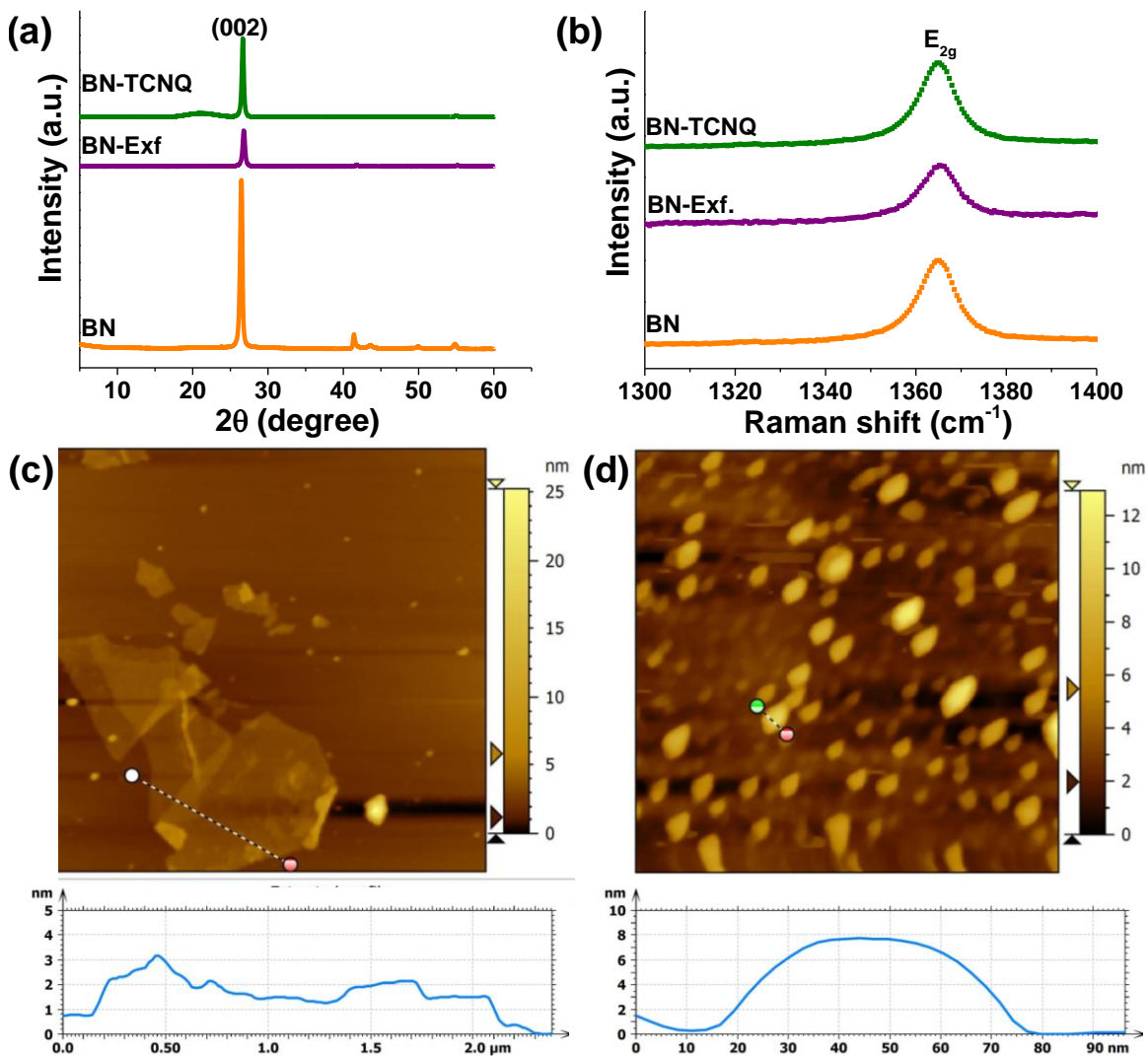


Figure 2: PXRD of BN (orange), BN-Exf. (violet), BN-TCNQ (green) (a), Raman spectra of BN (orange), BN-Exf. (violet), BN-TCNQ (green) (b), AFM image with height profile of BN-Exf. (c), AFM image with height profile of BN-TCNQ (d).

The thickness measured using AFM shows ~2.5 nm height of BN-Exf. (Figure 2c) indicating 8-9 layers¹¹ stacked together while the height profile of BN-TCNQ (Figure 2d) shows thickness of around ~8 nm which comprise of 22-24 layers stacked together. The increased height in BN-TCNQ driven by interaction between TCNQ and BN-Exf. results in precipitate formation.

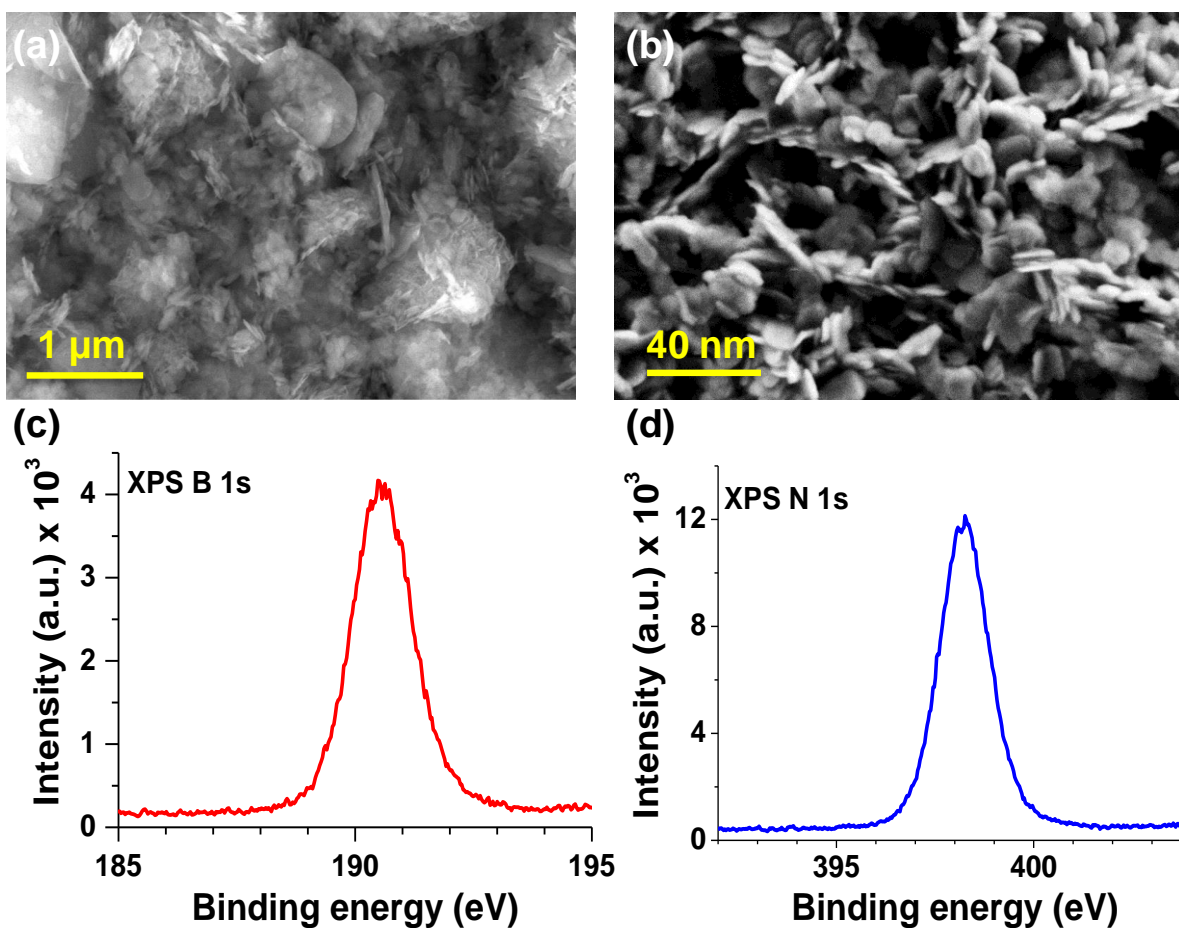


Figure 3: FESEM images of BN (a), BN-TCNQ (b), XPS of B 1s (c), N 1s (d).

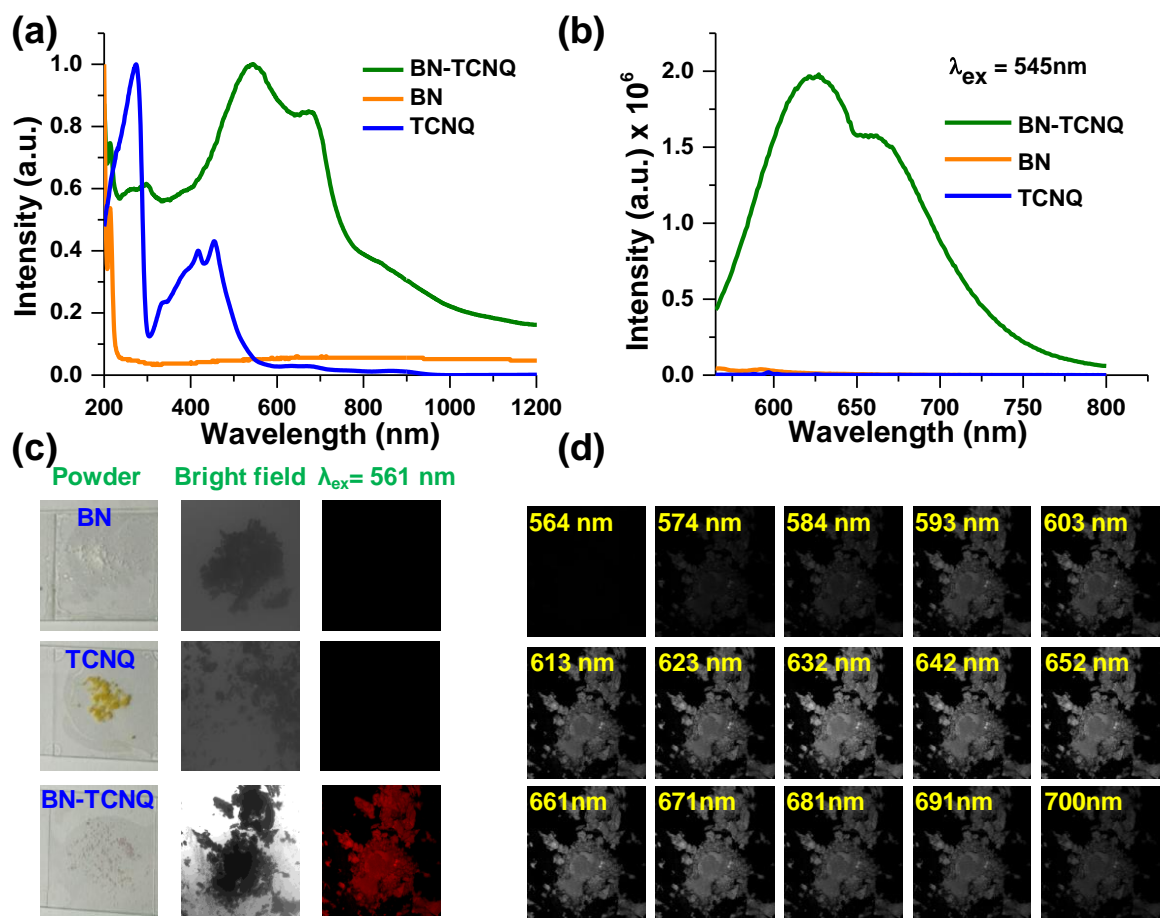


Figure 4: Solid state UV spectra of BN-TCNQ (green), BN (orange), TCNQ (blue) (a), Fluorescence spectra of BN-TCNQ (green), BN (orange), TCNQ (blue) (b), Powder of BN, TCNQ, BN-TCNQ, bright field image, PL image using laser of $\lambda_{ex} = 561$ nm (c), PL image using laser of $\lambda_{ex} = 561$ nm from 564 nm to 700 nm (d).

Drastic colour change of BN (white) to that of BN-TCNQ (pink) is a prime indication of charge transfer between BN and TCNQ.²⁷ The solid state UV spectra supports this observation, as BN-TCNQ is pink in colour so it should absorb in the range of green colour 495-570 nm. Indeed in solid state UV spectra (Figure 4a) we do observe the absorption peak at 545 nm. Apart from absorption peak at 545 nm we also get absorption at 260 nm, 300 nm, 660 nm, and 850 nm. The material has quiet broad range for absorption. Interestingly, the resultant BN-TCNQ hybrid shows Photoluminescence (PL) property which is absent in the parent compounds BN and TCNQ. The emission spectra (Figure 4b) show

two peaks at 625 nm and 661 nm corresponding to the absorption peak at 545 nm and 660 nm. The confocal microscope was used to record live image of PL. Green laser ($\lambda_{\text{ex}}=561$ nm) was used for excitation and the image (Figure 4c) was taken for all three samples BN, TCNQ and BN-TCNQ.

The parent compounds BN and TCNQ do not show any PL while we can see bright red emission in case of BN-TCNQ. Emission was collected in range from 564 to 720 nm at approximately 9.5 nm difference; all 15 images are shown in (Figure 4d).

TCNQ can exist into three different redox active forms such as TCNQ^0 , TCNQ^- , TCNQ^{2-} .²⁸ Now the question arises as to which form of TCNQ is present in BN-TCNQ. To check the form of TCNQ present in BN-TCNQ we characterized the BN-TCNQ using FTIR (Figure 5a). but it was difficult to trace TCNQ presence most probably due to very low loading of TCNQ. However we get some features (Figure 5a)(1235cm^{-1} , 1104cm^{-1} , 1279cm^{-1} , 1070cm^{-1}) but it is also does not match with TCNQ.

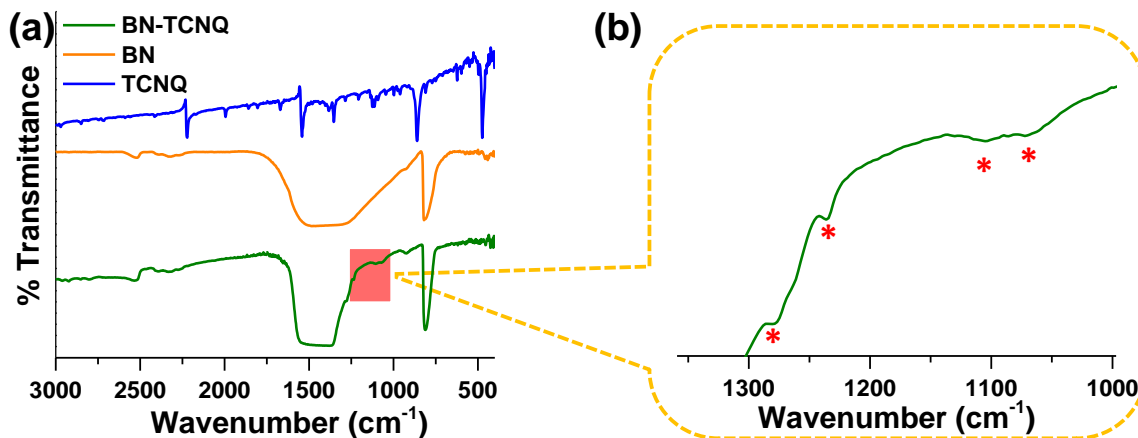


Figure 5: FTIR spectra of BN (orange), TCNQ (green), BN-TCNQ (green) (a), Zoom-in spectrum of BN-TCNQ ($1000\text{-}1300\text{ cm}^{-1}$) (b).

We took an alternative path to answer this question. The peculiar observation that colour change in BN-TCNQ supernatant solution is similar to that of TCNQ left in the solvent system comprising of DMF+IPA+Water in same volume ratio as in BN-TCNQ case, gives some hint that if it is possible to detect the change in TCNQ (DMF+Water+IPA), it could also possibly answer the question regarding which entity of TCNQ is really interacting with

BN. It is well known that TCNQ is a redox active moiety so we thought of recording the CV spectra (Figure 6) of TCNQ (DMF+IPA+Water) and compared it with TCNQ (DMF). Surprisingly the solution of TCNQ (DMF+IPA+Water) shows significant reduction in redox active peak compared to TCNQ (DMF) and vanishes after 2 days. This experiment suggests that TCNQ is getting converted to some species which is not redox active.

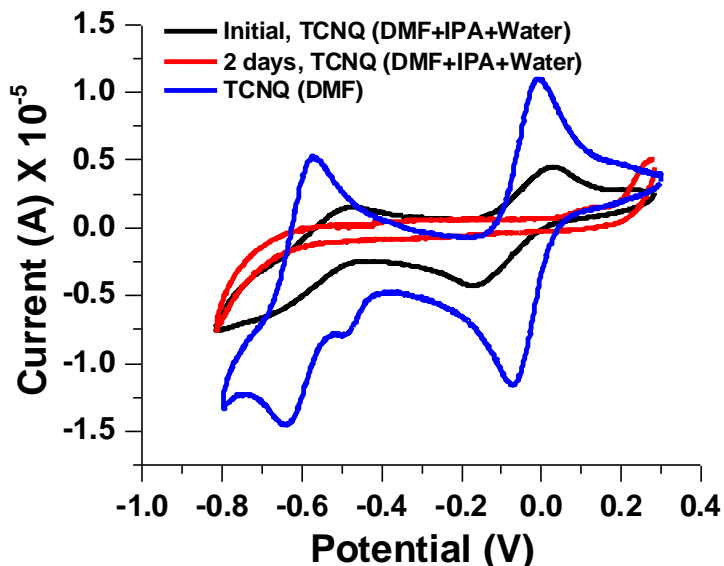
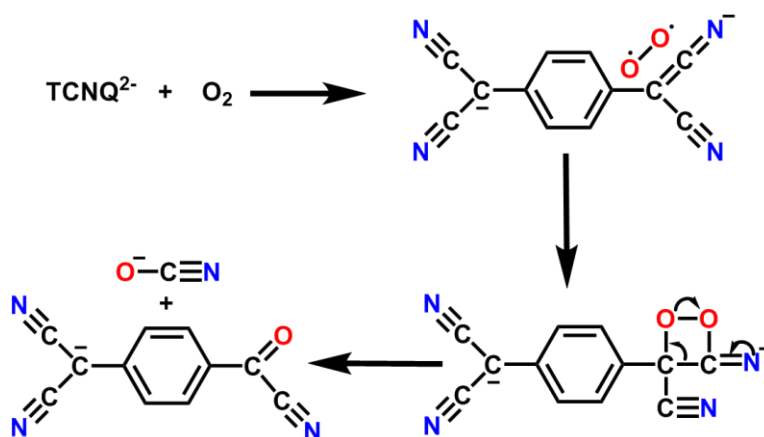


Figure 6: CV spectra of Initial TCNQ (DMF+IPA+Water) (black), 2 days TCNQ (DMF+IPA+Water) (red), TCNQ (DMF) (blue).

1.6 Mechanism

In search of the true entity interacting with BN we looked up the literature and figured out a new possibility of formation of an oxide decay product of TCNQ moiety to a species known as α - α -dicyano-p-toluoylcyanide (DCTC⁻) in the presence of water and oxygen.^{25, 28-29} To verify this point we performed number of experiments which would give us conclusive answer.

1.6.1 Conversion of TCNQ to DCTC⁻



Scheme 2: Schematic of conversion of TCNQ²⁻ to DCTC⁻

1.6.2 Experiment 1

We first checked the role of water. BN was exfoliated in DMF (instead of IPA+Water) and TCNQ was dissolved in three different solvent systems 1) DMF 2) IPA 3) DMF+IPA. The BN exfoliated in DMF was mixed with TCNQ in all three different solvent systems. A white precipitate settled at the bottom of all the three vials (Figure 7a). The supernatant solution in the present case did not show any colour change as observed in the previous case (Figure 1a) where supernatant colour changes to brown and pink precipitate was obtained. So we can conclude that water must have a critical role as the reaction was not successful in its absence.

1.6.3 Experiment 2

We took BN-Exf. (1.5 ml) and titrated it using the stock solution of TCNQ (1 mM, 10 ml DMF) with increasing concentration from 100 μ L to 1200 μ L and recorded the liquid state UV spectra (Figure 7b) from 200 nm to 1200 nm. The characteristic peaks correspond to around 400 nm of TCNQ, around 700 to 900 nm of TCNQ⁻ and around 330 and 488 nm of TCNQ²⁻. Apart from these peaks of TCNQ in its three different redox active forms, the peak at 480 nm is a clear signature of DCTC⁻.²⁹ Thus we can conclude that in DMF,

TCNQ exist in its all three forms and chemical conversion of TCNQ to DCTC⁻ takes place when it comes in contact with BN-Exf. solution due to the presence of water and atmospheric oxygen. Thus majorly DCTC⁻ is present in solution with some impurity of TCNQ.

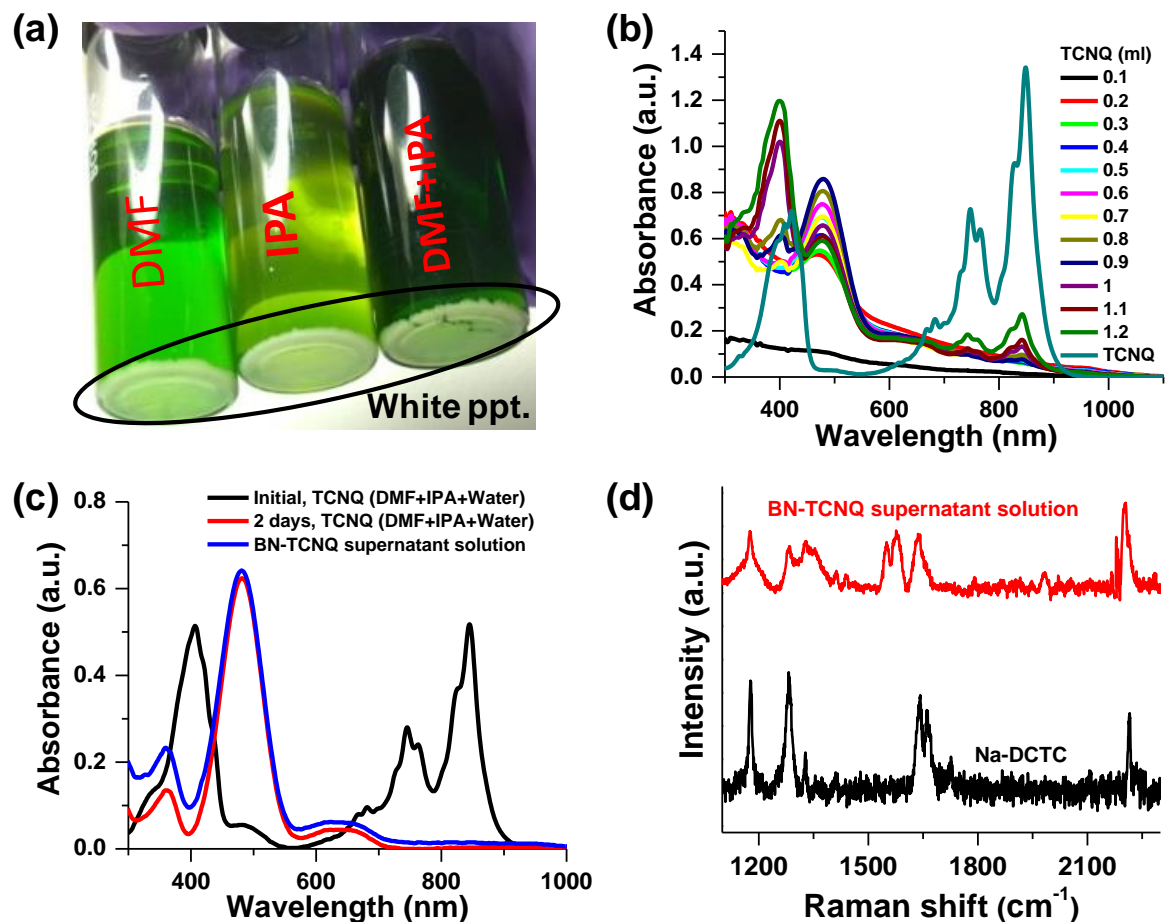


Figure 7: BN-Exf. (10 ml)+TCNQ (DMF)/(IPA)/DMF+IPA (10 ml)(white precipitate) (a), Liquid state UV-Vis. spectra of BN-Exf. (1.5 ml) + TCNQ (1mM) varied from 100 μ L to 1200 μ L compared with TCNQ (DMF) (b), Liquid state UV spectra of Initial TCNQ (DMF+IPA+Water) (black), 2 days TCNQ (DMF+IPA+Water) (red) (c), BN-TCNQ supernatant solution (blue) (d).

1.6.4 Experiment 3

The liquid state UV spectrum (Figure 7c) of TCNQ (DMF+IPA+Water) initially changes completely after 2 days and a new intense peak at 480 nm appeared which matches with

BN-TCNQ supernatant solution, indicating that oxidative decay product of TCNQ to DCTC⁻ is not governed by BN. It is water and oxygen that are responsible for conversion, after which DCTC⁻ interacts with BN.

1.6.5 Experiment 4

We have prepared Na-DCTC as mentioned in experimental section and collected its Raman spectra.³⁰ The Raman spectra (Figure 7d) of BN-TCNQ supernatant solution matches with the Na-DCTC. So majorly DCTC⁻ species is present in the solution.

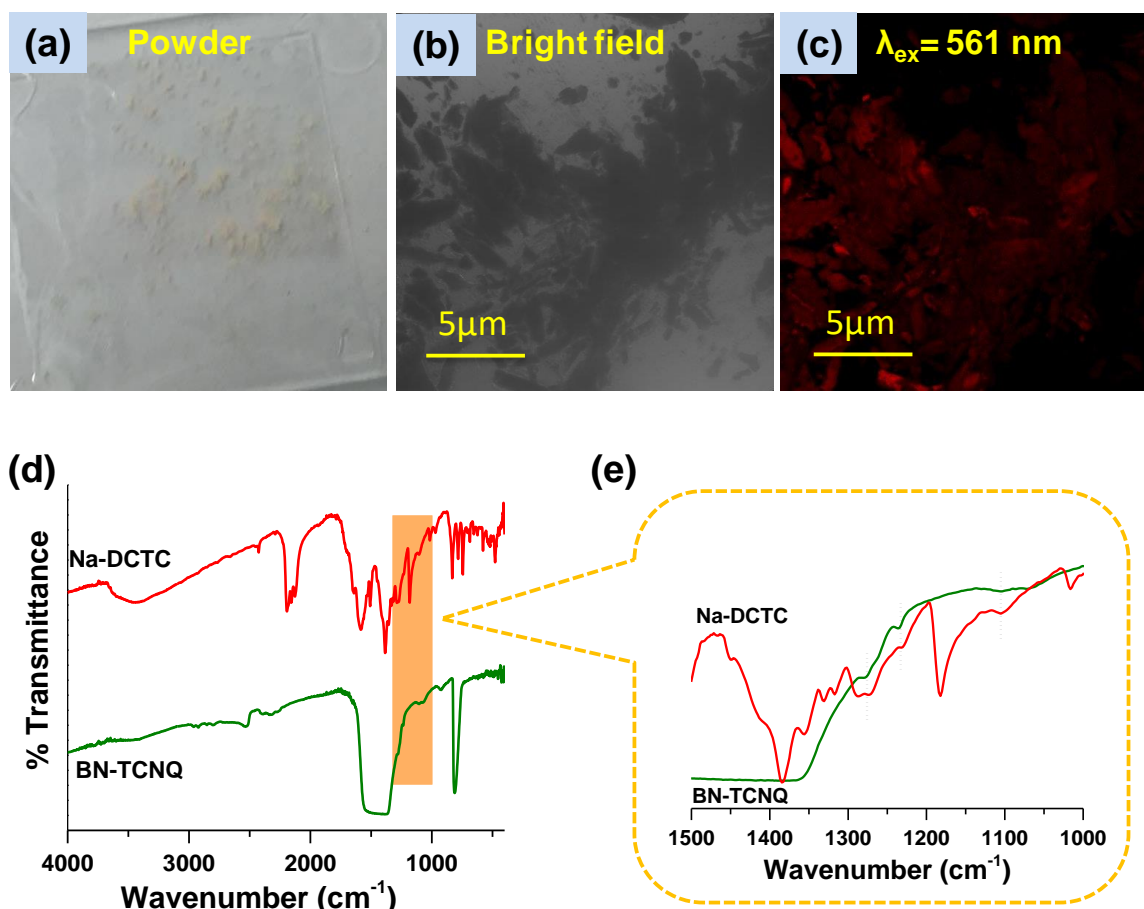


Figure 8: BN-DCTC powder, Bright field image, PL image with $\lambda_{ex} = 561$ nm (a-c), FTIR spectra of BN-TCNQ (green) , Na-DCTC (red) (d), FTIR zoom part of BN-TCNQ (green), Na-DCTC (red) from 1000 cm^{-1} to 1500 cm^{-1} (e).

1.6.6 Experiment 5

If DCTC⁻ species forms via chemical conversion of TCNQ and if it is the only species interacting with BN, we could synthesize it directly and add it to the BN-Exf. and check the PL effect. Indeed after synthesizing BN-DCTC as mentioned in the experimental section (1.2.5) above and on checking its confocal images the results were similar suggesting the formation of DCTC species that is responsible for PL effect. (Figure 8 a, b, c).

All the above five experiments carried out clearly suggest that TCNQ (DMF) present in all three redox forms gets converted to DCTC⁻ as it comes in contact with BN-Exf. (IPA+water) due to water. Only after this conversion the DCTC⁻ interacts with BN system to form a pink precipitate. To further support this argument we analyzed the FTIR spectra (Figure 8 d, e) of BN-TCNQ and Na-DCTC. There are few peaks which are common in (1235cm⁻¹, 1279cm⁻¹, 1104cm⁻¹) suggesting the presence of DCTC⁻. The peak at 1235cm⁻¹ corresponds to enolate character of carbonyl group present in DCTC⁻.

We further performed some experiments such as concentration dependent and temperature dependent studies as well as laser bleaching effect to get more insight –

1.7.1 Concentration dependent studies

BN-Exf. (10ml) was taken and TCNQ (10 ml DMF) with varying concentration (1 mM, 2 mM, 3 mM, 5 mM, and 10 mM) (Figure 9 a, b, c) were used. Upon mixing, we concluded that the yield of BN-TCNQ is maximum when the concentration of TCNQ is 2 mM. Upon increasing the concentration further, TCNQ itself gets precipitated out to form impurity along with precipitate (BN-TCNQ).

1.7.2 Temperature dependent studies

Next question we wanted to answer was whether we could play with kinetics of the reaction using temperature as a driving force so that instead of taking weeks for the BN-TCNQ formation the product could be obtained in a few hours. Keeping all experimental procedures same, we kept the BN-TCNQ solution at 120 °C for 6 hr. We obtained the

precipitate (Figure 9 d, e, f) and recorded its confocal images, we observed the same PL effects present here as well. Hence we can push the reaction at a faster rate using high temperature condition.

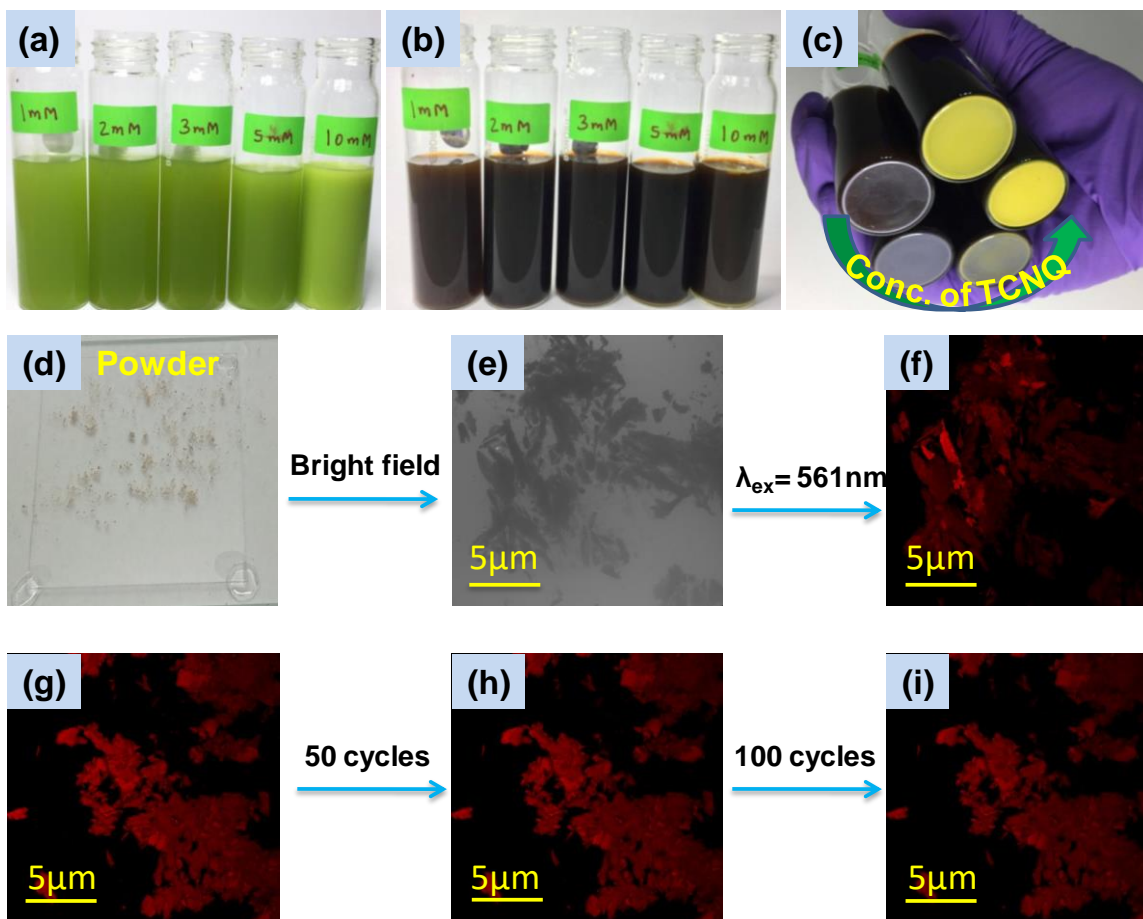


Figure 9: BN-Exf. (10 ml) + TCNQ (10 ml DMF) (1 mM, 2mM, 3mM, 5mM, 10mM) (a-c), BN-TCNQ synthesis at 120 °C, Powder of BN-TCNQ (a), Bright field image (b), PL image (c)

1.7.3 Laser bleaching effect

A number of fluorophores get damaged due to optical heating when laser is used for excitation multiple times. To check the stability of our material we recorded the confocal image (Figure 9 g, h, i) of BN-TCNQ at difference of 2 min for 100 cycles.

	Initial	50 cycles	100 cycles
CFCT	459316	417977	408791

Interestingly, the calculation of CFCT (using formula given below) tells us that our material retains more than 80% of emission even after 100 cycles.

$$\text{CFCT} = (\text{Integrated density}) - (\text{area of selected region} \times \text{mean value of background})$$

1.8 Electrical Measurements

The electrical measurements (Figure 10a) of BN and BN-TCNQ were performed in two probe station. The electrical resistance of BN was in order of $10^{14} \Omega$, while the resistance of BN-TCNQ is $10^{12} \Omega$. The decrease in electrical resistance is attributed to lowering of band gap (Figure 10b)

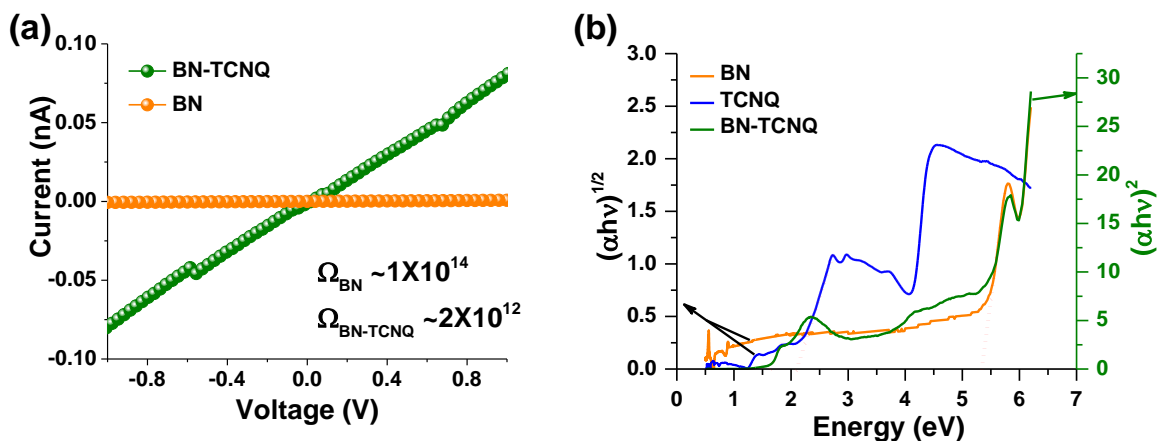


Figure 10: DC conductivity measurement using Two probe I-V, BN (orange), BN-TCNQ (green) (a), Tauc plot of BN (orange), TCNQ (blue), BN-TCNQ (green) (b).

1.9 Conclusion

In conclusion, for the first time we have synthesized a BN-TCNQ hybrid and obtained the interesting PL property which was absent in the parent compounds BN and TCNQ. The detail investigation revealed that TCNQ can exist in its three redox active form TCNQ^0 , TCNQ^- , TCNQ^{2-} , however, these are not the actual entities which interacts with BN and produces complex with PL property. A chemically converted form of TCNQ known as DCTC^- is interacts with BN and commits PL activity. The particular choice of solvent system (DMF+IPA+water) realized to be the crucial step in order to get the DCTC^- , where the water and atmospheric oxygen plays a key role. It was very difficult to detect DCTC^- in the BN-TCNQ powder, possibly due to very low loading of DCTC^- , therefore, various spectroscopic and electrochemical techniques were applied on supernatant solution and indirectly justified the DCTC^- formation in the complex. We have also synthesized Na-DCTC material externally and reacted with exfoliated BN (BN-Exf). Remarkably, the resulted product showed PL phenomenon, therefore, supported our observation on BN-TCNQ. Our concept of molecular doping can turn on PL in BN nanosheets and mimicking the similar organic molecule as DCTC^- can cover the whole visible range from red, green to blue. Theoretical calculation is needed further to support our observations.

2.0 Bibliography

- [1] Novoselov, K.; Mishchenko, A.; Carvalho, A.; Neto, A. C., 2D Materials and Van Der Waals Heterostructures. *Science* **2016**, *353*, 9439-9451.
- [2] Zhang, K.; Feng, Y.; Wang, F.; Yang, Z.; Wang, J., Two Dimensional Hexagonal Boron Nitride (2D-hBN): Synthesis, Properties and Applications. *J. Mater. Chem. C* **2017**, *5*, 11992-12022.
- [3] Novoselov, K.; Jiang, D.; Schedin, F.; Booth, T.; Khotkevich, V.; Morozov, S.; Geim, A., Two-Dimensional Atomic Crystals. *Proc. Natl. Acad. Sci. U.S.A* **2005**, *102*, 10451-10453.
- [4] Gong, C.; Zhang, H.; Wang, W.; Colombo, L.; Wallace, R. M.; Cho, K., Band Alignment of Two-Dimensional Transition Metal Dichalcogenides: Application in Tunnel Field Effect Transistors. *Appl. Phys. Lett.* **2013**, *103*, 053513.
- [5] Novoselov, K. S.; Geim, A. K.; Morozov, S. V.; Jiang, D.; Zhang, Y.; Dubonos, S. V.; Grigorieva, I. V.; Firsov, A. A., Electric Field Effect in Atomically Thin Carbon Films. *science* **2004**, *306*, 666-669.
- [6] Saito, Y.; Nojima, T.; Iwasa, Y., Highly Crystalline 2D Superconductors. *Nat. Rev. Mater.* **2017**, *2*, 16094.
- [7] Zhu, W.; Park, S.; Yogeesh, M. N.; Akinwande, D., Advancements in 2d Flexible Nanoelectronics: From Material Perspectives to Rf Applications. *Flex. Print. Electro.* **2017**, *2*, 043001.
- [8] Mounet, N.; Gibertini, M.; Schwaller, P.; Campi, D.; Merkys, A.; Marrazzo, A.; Sohler, T.; Castelli, I. E.; Cepellotti, A.; Pizzi, G., Two-Dimensional Materials from High-Throughput Computational Exfoliation of Experimentally Known Compounds. *Nat. Nanotechnol.* **2018**, *1*.
- [9] Kim, J.; Kwon, S.; Cho, D.-H.; Kang, B.; Kwon, H.; Kim, Y.; Park, S. O.; Jung, G. Y.; Shin, E.; Kim, W.-G., Direct Exfoliation and Dispersion of Two-Dimensional Materials in Pure Water Via Temperature Control. *Nat. Commun.* **2015**, *6*, 8294-8302.
- [10] Yin, J.; Li, J.; Hang, Y.; Yu, J.; Tai, G.; Li, X.; Zhang, Z.; Guo, W., Boron Nitride Nanostructures: Fabrication, Functionalization and Applications. *Small* **2016**, *12*, 2942-2968.
- [11] Lei, W.; Mochalin, V. N.; Liu, D.; Qin, S.; Gogotsi, Y.; Chen, Y., Boron Nitride Colloidal Solutions, Ultralight Aerogels and Freestanding Membranes through One-Step Exfoliation and Functionalization. *Nat. Commun.* **2015**, *6*, 8849-8856.
- [12] Tran, T. T.; Bray, K.; Ford, M. J.; Toth, M.; Aharonovich, I., Quantum Emission from Hexagonal Boron Nitride Monolayers. *Nat. Nanotechnol.* **2016**, *11*, 37-41.
- [13] Museur, L.; Anglos, D.; Petitet, J.-P.; Michel, J.-P.; Kanaev, A. V., Photoluminescence of Hexagonal Boron Nitride: Effect of Surface Oxidation under UV-Laser Irradiation. *J. Lumin.* **2007**, *127*, 595-600.
- [14] Choi, S.; Tran, T. T.; Elbadawi, C.; Lobo, C.; Wang, X.; Juodkazis, S.; Seniutinas, G.; Toth, M.; Aharonovich, I., Engineering and Localization of Quantum Emitters in Large Hexagonal Boron Nitride Layers. *ACS Appl. Mater. Interfaces* **2016**, *8*, 29642-29648.
- [15] Chejanovsky, N.; Rezai, M.; Paolucci, F.; Kim, Y.; Rendler, T.; Rouabeh, W.; Fávaro de Oliveira, F.; Herlinger, P.; Denisenko, A.; Yang, S., Structural Attributes and Photodynamics of Visible Spectrum Quantum Emitters in Hexagonal Boron Nitride. *Nano Lett.* **2016**, *16*, 7037-7045.
- [16] Tran, T. T.; Zachreson, C.; Berhane, A. M.; Bray, K.; Sandstrom, R. G.; Li, L. H.; Taniguchi, T.; Watanabe, K.; Aharonovich, I.; Toth, M., Quantum Emission from Defects in Single-Crystalline Hexagonal Boron Nitride. *Phys. Rev. Appl.* **2016**, *5*, 034005.
- [17] Tawfik, S. A.; Ali, S.; Fronzi, M.; Kianinia, M.; Tran, T. T.; Stampfl, C.; Aharonovich, I.; Toth, M.; Ford, M. J., First-Principles Investigation of Quantum Emission from hBN Defects. *Nanoscale* **2017**, *9*, 13575-13582.
- [18] Radhakrishnan, S.; Das, D.; Samanta, A.; Carlos, A.; Deng, L.; Alemany, L. B.; Weldeghiorghis, T. K.; Khabashesku, V. N.; Kochat, V.; Jin, Z., Fluorinated h-BN as a Magnetic

Semiconductor. *Sci. Adv.* **2017**, *3*, e1700842.

[19] Weng, Q.; Kvashnin, D. G.; Wang, X.; Cretu, O.; Yang, Y.; Zhou, M.; Zhang, C.; Tang, D. M.; Sorokin, P. B.; Bando, Y., Tuning of the Optical, Electronic, and Magnetic Properties of Boron Nitride Nanosheets with Oxygen Doping and Functionalization. *Adv. Mater.* **2017**, *29*.

[20] Peimyoo, N.; Yang, W.; Shang, J.; Shen, X.; Wang, Y.; Yu, T., Chemically Driven Tunable Light Emission of Charged and Neutral Excitons in Monolayer WS₂. *ACS Nano* **2014**, *8*, 11320-11329.

[21] Mouri, S.; Miyauchi, Y.; Matsuda, K., Tunable Photoluminescence of Monolayer MoS₂ via Chemical Doping. *Nano Lett.* **2013**, *13*, 5944-5948.

[22] Tang, Q.; Zhou, Z.; Chen, Z., Molecular Charge Transfer: A Simple and Effective Route to Engineer the Band Structures of BN Nanosheets and Nanoribbons. *J. Phys. Chem. C* **2011**, *115*, 18531-18537.

[23] Zhang, R.; Li, B.; Yang, J., A First-Principles Study on Electron Donor and Acceptor Molecules Adsorbed on Phosphorene. *J. Phys. Chem. C* **2015**, *119*, 2871-2878.

[24] Shen, J.; He, Y.; Wu, J.; Gao, C.; Keyshar, K.; Zhang, X.; Yang, Y.; Ye, M.; Vajtai, R.; Lou, J., Liquid Phase Exfoliation of Two-Dimensional Materials by Directly Probing and Matching Surface Tension Components. *Nano Lett.* **2015**, *15*, 5449-5454.

[25] Gossel, M. C.; Duke, A. J.; Hibbert, D. B.; Lewis, I. K.; Seddon, E. A.; Horton, P. N.; Weston, S. C., An Investigation of the Factors That Influence the Decomposition of 7, 7, 8, 8 - Tetracyanoquinodimethane (TCNQ) and its Salts to, and Structural Characterization of, the α , α -Dicyano-p-Toluoylcyanoide Anion. *Chem. Mater.* **2000**, *12*, 2319-2323.

[26] Feigelson, B. N.; Bermudez, V. M.; Hite, J. K.; Robinson, Z. R.; Wheeler, V. D.; Sridhara, K.; Hernández, S. C., Growth and Spectroscopic Characterization of Monolayer and Few-Layer Hexagonal Boron Nitride on Metal Substrates. *Nanoscale* **2015**, *7*, 3694-3702.

[27] Zhang, M.; Yao, W.; Lv, Y.; Bai, X.; Liu, Y.; Jiang, W.; Zhu, Y., Enhancement of Mineralization Ability of C₃N₄ via a Lower Valence Position by a Tetracyanoquinodimethane Organic Semiconductor. *J. Mater. Chem. A* **2014**, *2*, 11432-11438.

[28] Le, T. H.; Nafady, A.; Qu, X.; Bond, A. M.; Martin, L. L., Redox and Acid-Base Chemistry of 7, 7, 8, 8-Tetracyanoquinodimethane, 7, 7, 8, 8-Tetracyanoquinodimethane Radical Anion, 7, 7, 8, 8-Tetracyanoquinodimethane Dianion, and Dihydro-7, 7, 8, 8-Tetracyanoquinodimethane in Acetonitrile. *Anal. Chem.* **2012**, *84*, 2343-2350.

[29] Cehak, A.; Chyla, A.; Radomska, M.; Radomski, R., The Influence of Water and Oxygen on Stability of TCNQ Solution in Acetonitrile. *Mol. Cryst. Liq. Cryst.* **1985**, *120*, 327-331.

[30] Harris, M.; Hoagland, J.; Mazur, U.; Hips, K., Raman and Infrared Spectra of Metal Salts of A, A-Dicyano-P-Toluoylcyanoide: Non-Resonant Raman Scattering in Tetracyano-p-Quinodimethanide. *Vib. Spectrosc.* **1995**, *9*, 273-277.